Role of dopamine in reward expectation and predictability during execution of action sequences

AUTHORS

Robin Magnard[1]; Yifeng Cheng[1,3]; Joanna Zhou[1]; Haley Province[1]; Nathalie Thiriet[4]; Patricia H. Janak[1,2,3]; Youna Vandaele[1,4]

AFFILIATIONS

[1]Department of Psychological and Brain Sciences, Krieger School of Arts and Sciences, Johns Hopkins University, Baltimore, MD.
[2]Solomon H. Snyder Department of Neuroscience, Johns Hopkins School of Medicine, Johns Hopkins University, Baltimore, MD.
[3]Kavli Neuroscience Discovery Institute, Johns Hopkins University, Baltimore, MD.
[4]Université de Poitiers, INSERM, U-1084, Laboratoire des Neurosciences Expérimentales et Cliniques, Poitiers, France.

CORRESPONDENCE

Dr. Youna Vandaele, Université de Poitiers, INSERM, U-1084, Laboratoire des Neurosciences Expérimentales et Cliniques, Poitiers, France.

Phone: +33782507731

Email address: youna.vandaele@univ-poitiers.fr

Dr. Robin Magnard, Department of Psychological and Brain Sciences, Johns Hopkins University, Baltimore, MD, USA.

Phone: 410-516-7994

Email address: robin.magnard@jhu.edu

ABSTRACT:

Reward-associated cues serve different functions depending on whether they precede or terminate action sequences. Cues that precede action sequences and signal opportunity for reward could serve as GO signals to initiate the sequence, whereas sequence termination cues could serve as response feedback by signaling reward delivery. Reward expectation during sequence execution depends on these cues and might condition whether behavior is habitual or goal-directed. However, it remains unknown how sequence initiation and termination cues differentially affect reward expectation and contribute to habit learning. Further, while mesolimbic dopamine plays a key role in cue-induced reward expectation and sequence learning, how dynamic changes in dopamine signals differ depending on the response strategy is unclear. Here, we determined how mesolimbic DA signals change over training during cue-mediated sequence learning, depending on the type of cue and the nature of behavioral control. We found sequence initiation and termination cues differentially affect reward expectation during action sequences, with the termination cue contributing to habit and automaticity. Distinct response strategies induced by sequence initiation and termination cues induced differential changes in mesolimbic DA signals that captured variations in reward expectation along sequence execution. Notably, habit-like behavior induced by the sequence termination cue was associated with a rapid shift in DA signals from reward retrieval to the cue. This habit-like behavior was reflected in behavioral inflexibility and attenuated DA reward prediction error signals. Finally, using optogenetics, we provide evidence that phasic DA activity elicited by the sequence termination cue is critical for the development of habit-like behavior.

KEYWORDS: Dopamine; Nucleus Accumbens; Ventral Tegmental Area; Habit; Behavioral Chunking; Inflexibility; Reward Prediction Error

INTRODUCTION

The definition of habit involves an absence of reward expectation during reward-seeking behavior [1]. Indeed, although habits are commonly defined as actions controlled by stimulus-response associations, they are predominantly identified as an absence of goal-directed control (i.e. insensitivity to outcome devaluation and contingency degradation) [2,3]. The definition and description of habit have been extended to include important features such as rapid action execution, the formation of chunked action sequences, and action inflexibility [4–6]. Interestingly, it has been suggested that when individual actions are chunked into behavioral units, they are automatically executed in absence of reward expectation until completion of the behavioral sequence [7–10].

Previous findings reveal the importance of reward predictability in habit learning [11–16], either by making stimulus-response associations more explicit (such as in instrumental tasks with discriminative stimuli) and/or by reducing attentional demand during execution of behavior. For instance, we have shown that in a discrete-trials procedure, the lever insertion and retraction bracketing each trial promote habit, automaticity, and behavioral chunking [11,12,17]. However, it is unclear whether these processes can be attributed to the insertion of the lever, which signals distal reward availability and opportunity to respond, or its retraction, which signals proximal reward delivery. For instance, the lever insertion cue could promote stimulus-response habit by signaling the contextual conditions in which responses would result in reward delivery. In contrast, the lever retraction cue could serve as response feedback favoring habit by alleviating requirements for action monitoring. How these distinct reward-related cues affect reward expectation and contribute to habit and behavioral chunking remains unknown.

Changes in reward expectation mediated by reward-predictive cues are encoded by midbrain dopamine (DA) neurons [18,19]. Indeed, numerous studies suggest that midbrain DA neurons signal reward prediction error (RPE) in Pavlovian and operant conditioning [19–26], and that this RPE signal may serve to confer motivational value to actions and reward-predictive cues [22,26]. DA release has also been investigated in the context of spatial navigation and sequence learning [27–30]. Evidence indicates that across sequence learning, mesolimbic DA signals in the nucleus accumbens (NAc) backpropagate from the reward and the action sequence to the most distal reward-predictive cue. Furthermore, it has been shown that mesolimbic DA signals predict performance of action sequences [27,28] and flexibly scale with distance to reward to sustain motivation toward the goal [31,32]. However, habitual control was not investigated in these studies. Therefore, it remains unclear how DA signals at action and reward-predictive cues change along execution of the behavioral sequence when behavior is goal-directed and when it becomes automated and habitual. In this study, we sought to address these questions by determining how mesolimbic DA signaling changes over training during cue-mediated sequence learning depending on the type of cue (sequence initiation cue versus sequence termination cue) and the nature of behavioral control (goal-directed versus habit-like).

RESULTS

Sequence termination cues promote habit-like behavior

To discern the roles of sequence initiation cues and sequence termination cues in instrumental behavior, we designed two tasks in which the lever could either serve as the cue that triggers the initiation of the sequence of actions (i.e. lever insertion) or as the cue that signals its completion (i.e. lever retraction). We assessed different features of habit, namely, action automaticity, behavioral chunking, and insensitivity to outcome devaluation.

After initial training under a free-operant uncued fixed-ratio 5 (FR5) schedule, rats were trained in one of two procedures designed to isolate the impact of the sequence initiation and termination cues (**Fig. 1a-b**). The first group of rats was trained in the lever insertion fixed-ratio 5 (LI5) task in which trials began with insertion of the lever. Rats were then required to complete a sequence of 5 lever presses to obtain the reward (0.1 ml of sucrose 20%). In this LI5 task, reward delivery was not signaled by lever retraction, which occurred at a random interval during reward retrieval (**Fig. 1a**). The second group of rats was trained in the lever retraction fixed-ratio 5 (LR5) task in which reward delivery was directly signaled by lever retraction, occurring at completion of five lever presses. However, the lever insertion cue was not relevant for signaling trial onset since it occurred during reward retrieval (**Fig. 1b**). These procedures allowed us to isolate and evaluate the behavioral impact of the lever insertion cue in the LI5 task and the lever retraction cue in the LR5 task.

Task differences rapidly emerged during training with a greater increase in response rate for rats trained in the LR5 task (**Fig. 1c**). Rats trained in the LR5 task exhibited a higher response rate in the last LR5 session compared to the first LR5 session and compared to the last LI5 session (**Fig. 1d**). The heightened response rate in the LR5 group was accompanied by a reduction in inter-press interval (IPI) duration. While the distribution of inter-press interval (IPI) was comparable between tasks on the first session, with a similar proportion of IPIs shorter than 0.5-s (**Fig. 1e**), LR5 rats had a greater proportion of shorter IPIs on the last training session as compared with LI5 rats (**Fig. 1f**). These results suggest greater action automaticity in the LR5 task isolating lever retraction at the end of sequence completion, compared to the LI5 task isolating lever insertion prior to sequence initiation.

Congruent with these observations, in the LR5 task, rats rapidly learned to complete the required ratio by pressing on the lever until its retraction. This resulted in a drastic decrease across LR5 sessions in the likelihood of checking the port during sequence execution (**Fig. 1g**). In contrast, in the LI5 task where there was no sequence termination cue, rats checked the reward port regularly, with port checking probability remaining near the maximum possible across sessions (**Fig. 1g-h**). The rapid increase in response rate concomitant with suppression of port checking during sequence execution in the LR5 task suggests that rats learned to concatenate individual lever presses into single behavioral sequences, a process referred to as behavioral chunking, executing the sequence without reward expectation until its completion. Indeed, rats in the LR5 group made a majority of short sequences (1-3 lever presses before port checking) during the first session (**Fig. 1i**) but learned to complete the full lever press sequence without checking the port by the end of training (**Fig. 1j**). In contrast, rats trained in the LI5 task showed no evidence of behavioral chunking across training, as they persisted in port checking after every few lever presses from the first (**Fig. 1i**) to the last (**Fig. 1j**) training session.

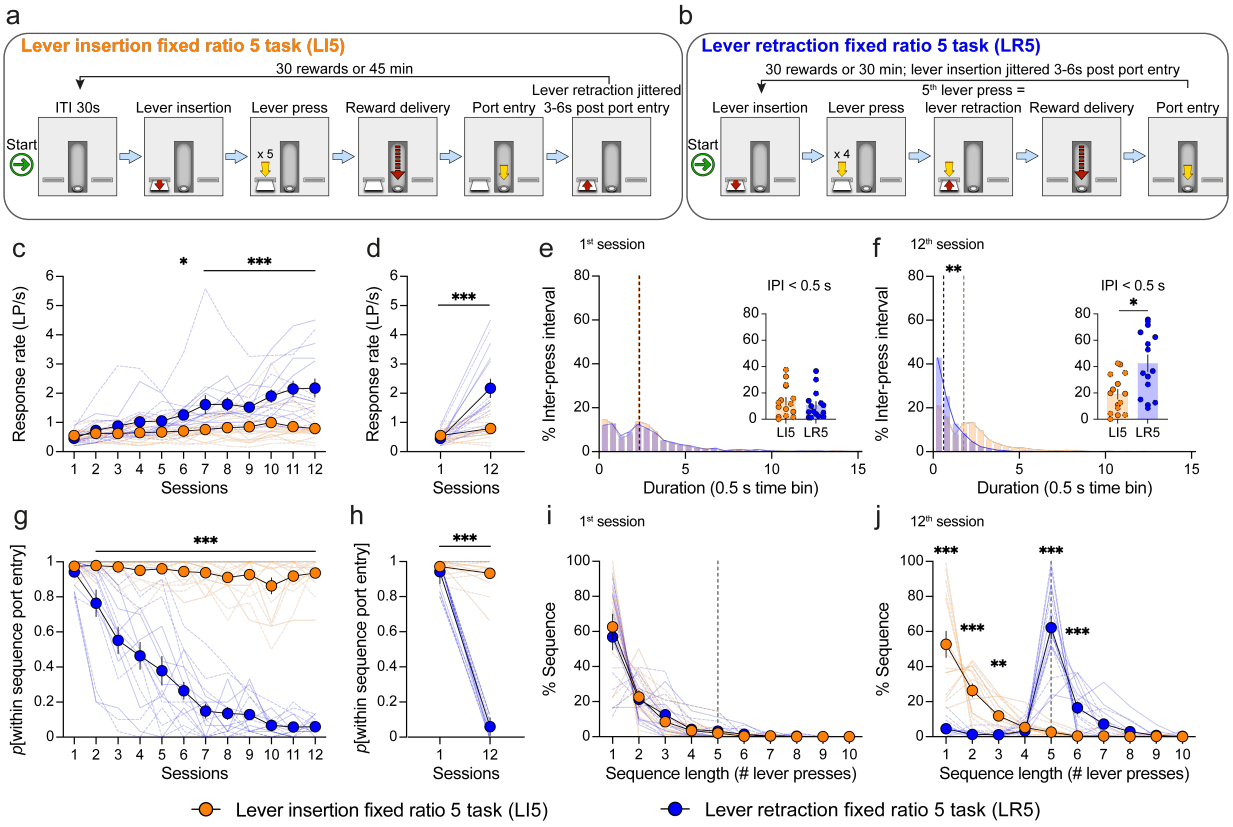

Figure 1. The lever retraction cue, but not the lever insertion cue, promotes action automaticity and behavioral chunking. (**a**) *Lever insertion fixed-ratio 5 (LI5) task design.* (**b**) *Lever retraction fixed-ratio 5 (LR5) task design.* (**c**) *Response rate in lever press per second (LP/s), within the lever press sequence during LI5/LR5 training sessions (three-way RM ANOVA, task effect:* $F_{1,26} = 10.2$, $p = 0.004$; *task x session interaction:* $F_{11,286} = 11.80$, $p < 0.001$; *task x session x sex interaction* $F_{11,286} = 2.74$, $p = 0.002$, *no task x sex interaction:* $F_{1,26} < 1$, $p = 0.58$; *no sex effect:* $F_{1,26} < 1$, $p = 0.98$; *Student Newman-Keuls post hoc pairwise comparison).* (**d**) *Response rate on the first versus last session in the LI5/LR5 tasks (three-way RM ANOVA, task x session interaction:* $F_{1,26} = 28.58$, $p < 0.001$; *no task x session x sex interaction F1,26 = 1.75, p = 0.19; Student Newman-Keuls post hoc pairwise comparison).* (**e**) *Frequency distribution of inter-press intervals (IPI) for the 1st LI5/LR5 session (Mann-Whitney Rank Sum t-test median comparison U = 455, p = 0.725). Insert panel: individual proportion of IPI under 0.5-s (two-way ANOVA no task effect:* $F_{1,30} < 1$, $p = 0.5$; *no task x sex interaction:* $F_{1,30} < 1$, $p = 0.95$). (**f**) *Frequency distribution of IPI for the 12th LI5/LR5 session (Mann-Whitney Rank Sum t-test median comparison U = 290, p = 0.007). Insert panel: individual proportion of IPI under 0.5-s (two-way ANOVA task effect:* $F_{1,30} = 10.6$, $p = 0.003$; *no task x sex interaction:* $F_{1,30} < 1$, $p = 0.40$; *Student Newman-Keuls post hoc pairwise comparison).* (**g**) *Probability to enter the port within the lever press sequence (within-sequence port entry) during training in LI5/LR5 tasks (three-way RM ANOVA, task effect:* $F_{1,26} = 231.3$, $p < 0.001$; *task x session interaction:* $F_{11,286} = 37.8$, $p < 0.001$; *no task x session x sex interaction* $F_{11,286} < 1$, $p = 0.98$; *Student Newman-Keuls post-hoc pairwise comparison).* (**h**) *Probability of within sequence port entry on the first versus last training session in the LI5/LR5 tasks (three-way RM ANOVA, task x session interaction:* $F_{1,26} = 801.7$, $p < 0.001$; *no task x session x sex interaction* $F_{1,26} < 1$, $p = 0.80$; *Student Newman-Keuls post hoc pairwise comparison).* (**i**) *Frequency distribution of sequence lengths during the first training session in the LI5/LR5 tasks. The grey dashed line represents the optimal sequence length of 5 lever presses (three-way RM ANOVA, no task effect:* $F_{1,26} < 1$, $p = 0.885$; *no task x sequence length interaction:* $F_{9,234} < 1$, $p =$

*0.96; no task x sequence length x sex interaction $F_{9,234}$ = 1.29, p = 0.24). (**j**) Frequency distribution of sequence length during the last training session in the LI5/LR5 tasks. The grey dashed line represents the optimal sequence length of 5 lever presses (three-way RM ANOVA, no task effect: $F_{1,26}$ < 1, p = 1; task x sequence length interaction: $F_{9,234}$ = 48.5, p < 0.001; no task x sequence length x sex interaction $F_{9,234}$ < 1, p = 0.67 Student Newman-Keuls post-hoc pairwise comparison). Data shown as mean ± SEM, superimposed with individual data point. LI5: n = 15 (7 males; 8 females); LR5: n = 15 (7 males; 8 females). Solid lines: males; dashed lines: females. *p < 0.05; **p < 0.01; ***p < 0.001.*

Task differences in action automaticity and behavioral chunking were associated with differences in sensitivity to sensory-specific satiety-induced outcome devaluation (**Suppl. Fig. 1**). Indeed, after only a few sessions, a higher proportion of rats showed insensitivity to devaluation (devaluation ratio ≤ 0) for the LR5 task compared to the LI5-task (**Suppl. Fig. 1**; 8/15 for LR5 task vs 1/15). We found no effect of sex on any of these performance variables. Taken together, these results show that the lever retraction cue, rather than the lever insertion cue, promotes habit-like behavior, characterized by action automaticity, behavioral chunking, and greater propensity to show insensitivity to outcome devaluation.

Distinct patterns of VTA DA neuron activity in response to cues and reward depending on response strategy

To determine if DA dynamics during behavioral sequence execution depend on cue-mediated reward expectation and prediction, we next used fiber photometry to examine ventral tegmental area (VTA) DA neuron activity across training in the LR5 and LI5 tasks. For selective recording of DA neurons, we expressed GCaMP6f in the VTA of tyrosine hydroxylase TH-Cre$^+$ rats, which allowed targeting of TH$^+$ DA neurons with 95% specificity (**Fig. 2a-c**). We replicated the differences in behavior observed in the two tasks (**Suppl. Fig. 2**). We observed no sex differences in behavior or neural activity and combined both sexes in the following analyses.

We monitored changes in DA neuron activity across trials in the LI5 and LR5 tasks at the lever insertion and retraction cues, at reward retrieval, and during lever presses. Changes in action automaticity and behavioral chunking occurred within the very first session in the LR5 task, with an increase in response rate and a decrease in port checking from the first 15 trials to the next 15 trials of the first session (**Suppl. Fig. 2b and f**). Thus, for both tasks, we analyzed changes in activity across 3 sets of 15 trials: the first 15 trials of the first session (trials 0-15), the second 15 trials of the first session (trials 16-30) and the last 15 trials of the last training session.

In the LI5 task, where the lever insertion cue signals opportunity to lever press for reward, there was an increase in DA neuron activity associated with the lever insertion cue (**Fig. 2d**), and after reward retrieval (**Fig. 2f**), with no change in either of these over repeated trials, and no obvious change at completion of the ratio (**Fig. 2e**). In contrast, in the LR5 task, where lever retraction serves as the cue for sequence completion and reward delivery, we observed rapid training-related changes in DA neuron activity, with reward signaling shifting to the lever retraction cue as learning progressed. While changes in DA neuron activity associated with the lever insertion cue were not statistically significant (**Fig. 2g**), we observed dynamic training-related changes in DA neuron activity at the end of the behavioral sequence (**Fig. 2h-i**). Specifically, from the first to the second 15 trials, the DA response to the lever retraction cue increased. In parallel, during the first 15 trials, DA neuron activity peaked during reward retrieval (**Fig. 2i**), with onset of this peak shifting over subsequent trials to before the port entry (**Fig. 2i**), likely corresponding to the lever retraction peak in **Fig. 2h**. Both the lever retraction cue and reward peaks of activity decreased with extended training in the LR5 task (**Fig 2h-i**; last 15 trials).

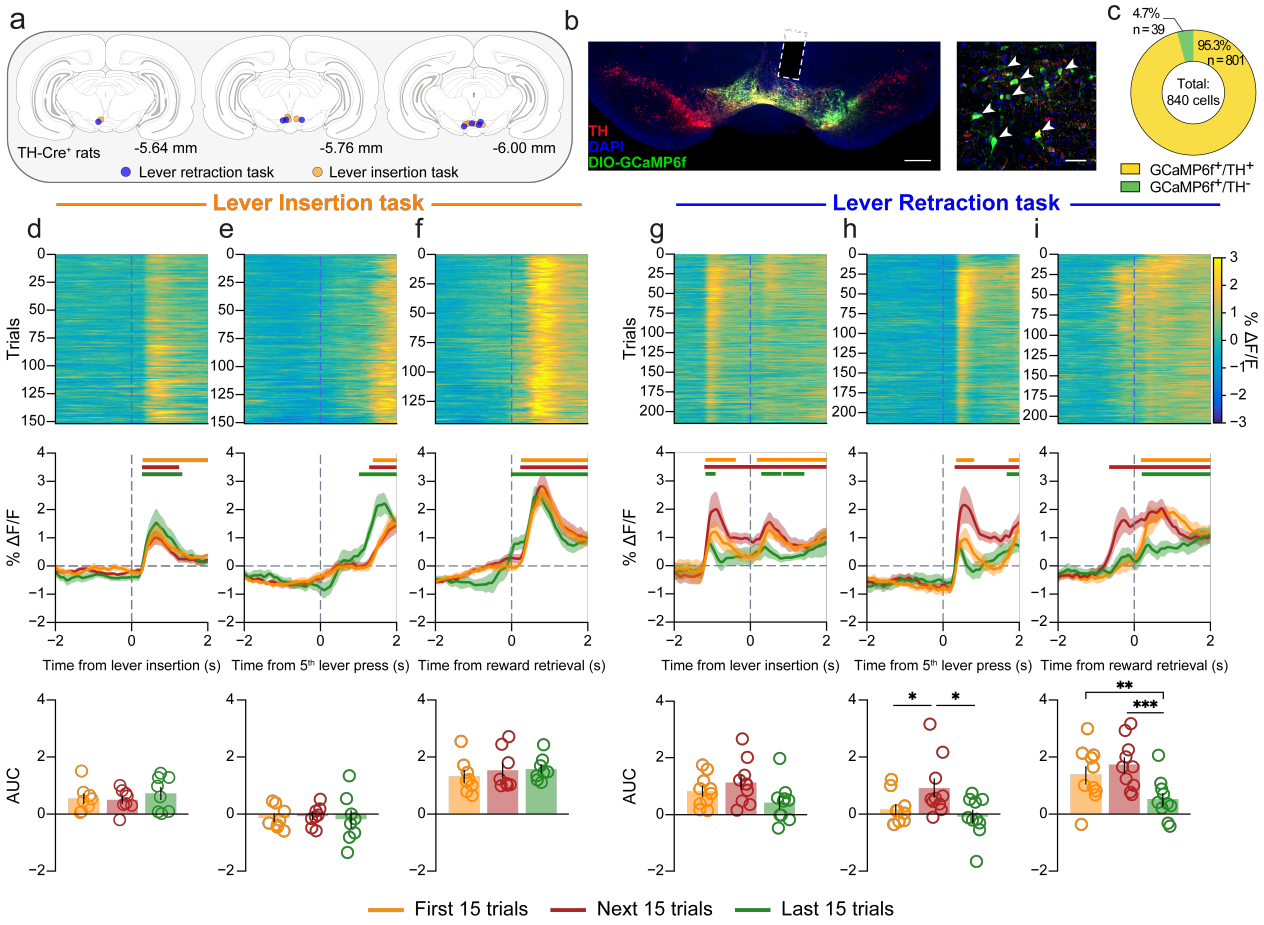

Figure 2. Distinct patterns of VTA dopamine neuronal phasic activity in response to cues and reward in the two tasks. *(**a**) Coronal sections showing location of optic fiber tips relative to Bregma for TH-Cre^{+} rats in LI5 and LR5 tasks. (**b**) Left panel: DIO-GCaMP6f was infused in the VTA of TH-Cre^{+} rats, and the optic fiber, represented with the white dash line, was implanted above the infusion site. Scale bar: 500 µm. Right panel: histology confirmation of DIO-GCaMP6f (green) and TH (red) co-expression (indicated by white arrows). Scale bar: 50 µm. (**c**) GCaMP6f virus is predominantly expressed in TH+ neurons. (**d**) Top panel: LI5 task heatmap displaying trial-by-trial dopamine neuron activity, averaged across rats, around lever insertion. Middle panel: phasic dopamine neuron activity around lever insertion averaged across rats and trials for the first 15 trials (orange line), the next 15 trials (red line) and the final 15 trials (green line) of training. Bottom panel: area under the curves (AUCs) for 0 to 1 seconds following lever insertion (two-way RM ANOVA, no trial x sex interaction $F_{2,12} < 1$, $p = 0.65$; no trial effect: $F_{2,12} < 1$, $p = 0.461$). (**e**) Same as d for the 5th lever press event in the LI5 task (two-way RM ANOVA, no trial x sex interaction $F_{2,12} < 1$, $p = 0.698$; no trial effect: $F_{2,12} < 1$, $p = 0.874$). (**f**) Same as d for reward retrieval in the LI5 task (two-way RM ANOVA, no trial x sex interaction $F_{2,12} < 1$, $p = 0.899$; no trial effect: $F_{2,12} = 1.92$, $p = 0.188$). (**g**) Same as d for lever insertion in the LR5 task (two-way RM ANOVA, no trial x sex interaction $F_{2,16} = 1.2$, $p = 0.31$; no trial effect: $F_{2,12} = 2.8$, $p = 0.09$). (**h**) Same as d for the 5th lever press in the LR5 task (two-way RM ANOVA, no trial x sex interaction $F_{2,16} > 1$, $p = 0.959$; trial effect: $F_{2,16} = 6.48$, $p = 0.008$; Unpaired two-tailed t-test post-hoc comparison). (**i**) Same as d for reward retrieval in the LR5 task (two-way RM ANOVA, no trial x sex interaction $F_{2,16} = 2.83$, $p = 0.08$; trial effect: $F_{2,16} = 25.33$, $p < 0.001$; Unpaired two-tailed t-test post-hoc comparison). Data shown as means ± SEM, superimposed with individual data point. LI5 n = 8 (3 males; 5*

*females); LR5 n = 10 (5 males; 5 females). Horizontal bars indicate significant deviation from baseline at 99% confidence level. *p < 0.05; **p < 0.01; ***p < 0.001.*

Distinct patterns of VTA DA neuron activity during lever press sequences between the two tasks

Analysis of changes in DA neuron activity across lever presses revealed intriguing task differences (**Fig. 3**). To compare activity after the lever press action, we examined the first 4 responses only as the 5th response is coupled to lever retraction in the LR5 task as shown above (**Fig. 2**). In the LI5 task, DA neuron activity associated with the initiation of the lever press sequence changed over time, with a peak of activity at the initiation of the sequence initially following the first lever press (first and next 15 trials) and progressively shifting to before the lever press (last 15 trials; **Fig. 3a**). Furthermore, DA neuron activity decreased as rats progressed in the execution of the sequence from the first to the fourth lever press (**Fig. 3e-f**), with an overall suppression immediately post-press during the last 15 trials (**Fig. 3a-d and g**).

In contrast, in the LR5 task, large modulations of DA activity around lever presses were not observed (**Fig. 3h-k**). Instead, a modest decrease in signal occurred across training (**Fig. 3l-n**). Similar patterns of DA neuron activity were observed during the first and last training sessions in the LI5 and LR5 tasks when the recorded signals were deconvoluted to isolate the neural responses associated with individual behavioral events (lever press, reward retrieval) while avoiding contamination from neighboring events (**Suppl. Fig. 3**; details in Online Methods).

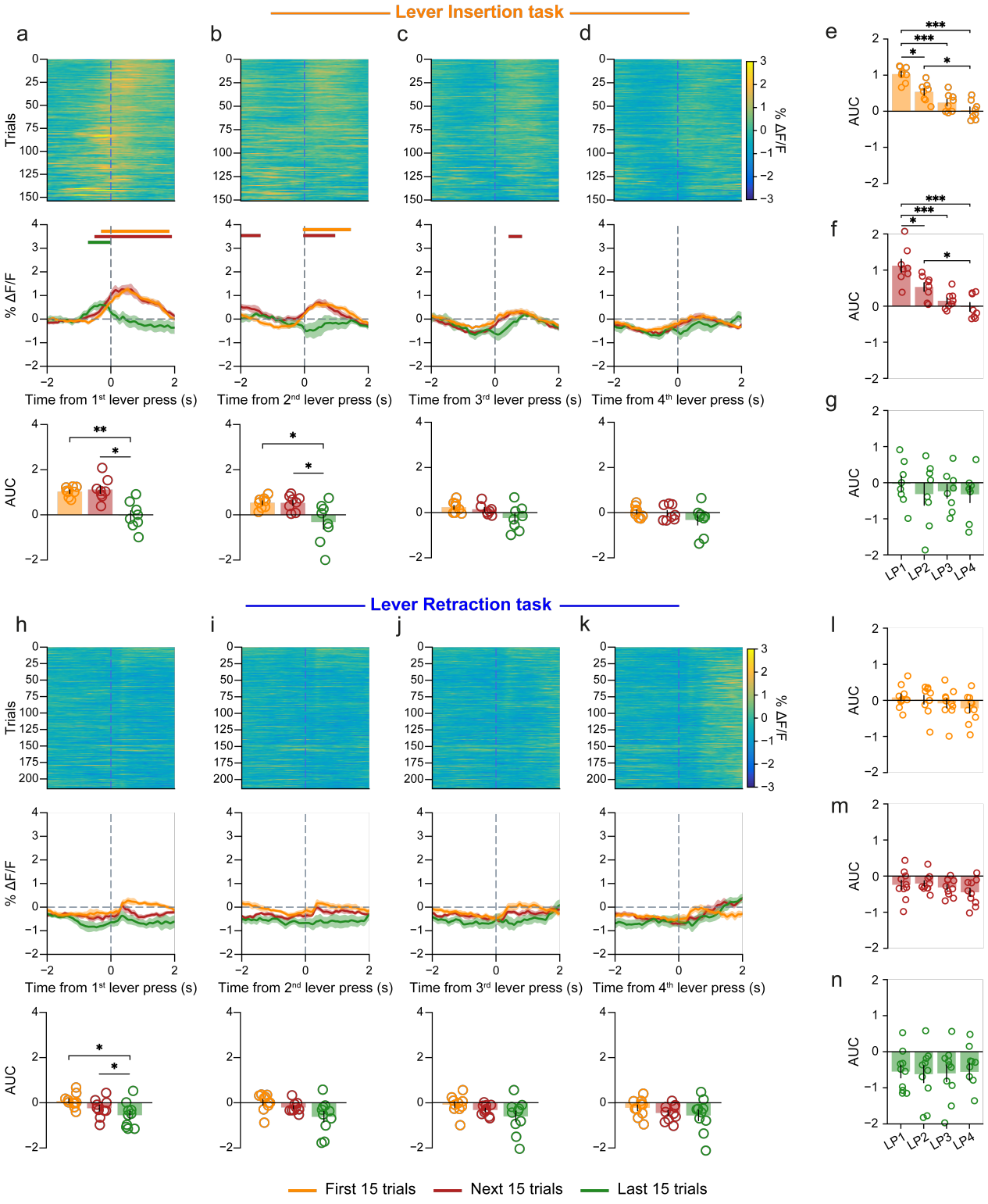

Figure 3. Distinct patterns of VTA DA neuronal activity during lever press sequences in the two tasks. *(**a-d**) Sequence of the first four lever presses for the LI5 task. The upper panel heatmaps illustrate trial-by-trial dopamine neuron activity, averaged across rat. The middle panel represents dopamine neuron activity averaged across rats and trials, delineated for the first 15 trials (orange line), the next 15 trials (red line), and the final 15 trials (green line) of the training*

*period. The bottom panel displays the area under the curves (AUCs) for the 0 to 1 seconds following the event. (**a**) 1st lever press (LP1; two-way RM ANOVA, no trial x sex interaction $F_{2,12}$ < 1, p = 0.788; trial effect: $F_{2,12}$ = 13.11, p < 0.001. Pairwise two-tailed t-test post-hoc comparison). (**b**) 2nd lever press (LP2; two-way RM ANOVA, no trial x sex interaction $F_{2,12}$ < 1, p = 0.508; trial effect: $F_{2,12}$ = 9.16, p = 0.003. Pairwise two-tailed t-test post-hoc comparison). (**c**) 3rd lever press (LP3; two-way RM ANOVA, no trial x sex interaction $F_{2,12}$ = 1.83, p = 0.201; trial effect: $F_{2,12}$ = 5.08, p = 0.025. Pairwise two-tailed t-test post-hoc comparison). (**d**) 4th lever press (LP4; two-way RM ANOVA, no trial x sex interaction $F_{2,12}$ = 1.02, p = 0.389; no trial effect: $F_{2,12}$ = 2.1, p = 0.164). (**e-g**) Area under the curves (AUCs) for the 0 to 1 seconds for the first four presses of the sequence in the LI5 task during the first 15 trials (**e**), the next 15 trials (**f**), and the final 15 trials (**g**) (two-way RM ANOVA, trial effect: $F_{2,14}$=10.12, p < 0.05; lever press effect: $F_{3,21}$ = 28.63, p < 0.0001; lever press x trial interaction $F_{6,42}$ = 5.77, p < 0.001. Pairwise two-tailed t-test post-hoc comparison). (**h to k**) same as (**a-d**) for the LR5 task. (**h**) 1st lever press (LP1; two-way RM ANOVA, no trial x sex interaction $F_{2,16}$ = 1.13, p = 0.345; trial effect: $F_{2,16}$ = 10.09, p = 0.001. Pairwise two-tailed t-test post-hoc comparison). (**i**) 2nd lever press (LP2; two-way RM ANOVA, no trial x sex interaction $F_{2,16}$ < 1, p = 0.863; trial effect: $F_{2,16}$ = 4.16, p = 0.03. Pairwise two-tailed t-test post-hoc comparison). (**j**) 3rd lever press (LP3; two-way RM ANOVA, no trial x sex interaction $F_{2,16}$ < 1, p = 0.453; no trial effect: $F_{2,16}$ = 2.09, p = 0.08). (**k**) 4th lever press (LP4; two-way RM ANOVA, no trial x sex interaction $F_{2,16}$ = 3.32, p = 0.06; no trial effect: $F_{2,16}$ = 1.98, p = 0.170). (**l-n**) same as (**e-g**) for the LR5 task (two-way RM ANOVA, trial effect: $F_{2,18}$ = 4.77, p < 0.05; no lever press effect: $F_{3,27}$ = 3.23, p = 0.08; no lever press x trial interaction $F_{6,54}$ = 1.25, p = 0.29. Pairwise two-tailed t-test post-hoc comparison). Data shown as means ± SEM, superimposed with individual data point. LI5 n = 8 (3 males; 5 females); LR5 n = 10 (5 males; 5 females). Horizontal bars indicate significant deviation from baseline at 99% confidence level. *p < 0.05; ***p < 0.001.*

The lever retraction cue promotes behavioral inflexibility, which is associated with attenuated RPE DA signals in the VTA

After training in the LR5 and LI5 tasks, the rats were tested in a single session using an omission schedule to evaluate their behavioral and dopaminergic responses to reversed instrumental contingencies. The omission procedures mirrored the task structure rats underwent during training. During the omission tests, all rats had to refrain from pressing the lever for 20 seconds to receive a reward. For the LI5 task, five presses on the lever resulted in omission of the reward but lever retraction was delayed until the port entry (**Fig. 4a**), while for the LR5 task, the fifth lever press resulted in omission of the reward and lever retraction (**Fig. 4b**).

During the omission tests, rats trained in the LR5 task exhibited a higher number of lever presses compared to rats trained in the LI5 task (**Fig. 4c**), indicating a reduced ability to adapt to the new contingencies relative to LI5-trained rats. This difference in behavioral flexibility was paralleled by differences in DA neuron activity. Neuronal activity differed between tasks at the port entry following ratio completion and omission of the reward (**Fig. 4f-g**), and the port entry following unexpected reward delivery upon successful response withholding (**Fig. 4h-i**). LI5 rats exhibited a robust decrease in DA neuron activity following omission of the reward (**Fig. 4f-g**) that was absent in LR5 rats. While DA activity increased in both groups following unexpected reward delivery, this was greater in LI5 rats (**Fig. 4f-g**). These differences in reward signals are unlikely to be attributed to different motor behavior as the mean latency to enter the port after reward omission (**Fig. 4d**) or delivery (**Fig. 4e**) does not differ in LR and LI rats.

These results suggest that following training in the LR5 task, rats are deficient in adapting to new instrumental contingencies and this deficiency is associated with attenuation of negative RPE signals following omission of expected reward, and positive RPE signals following unexpected reward delivery.

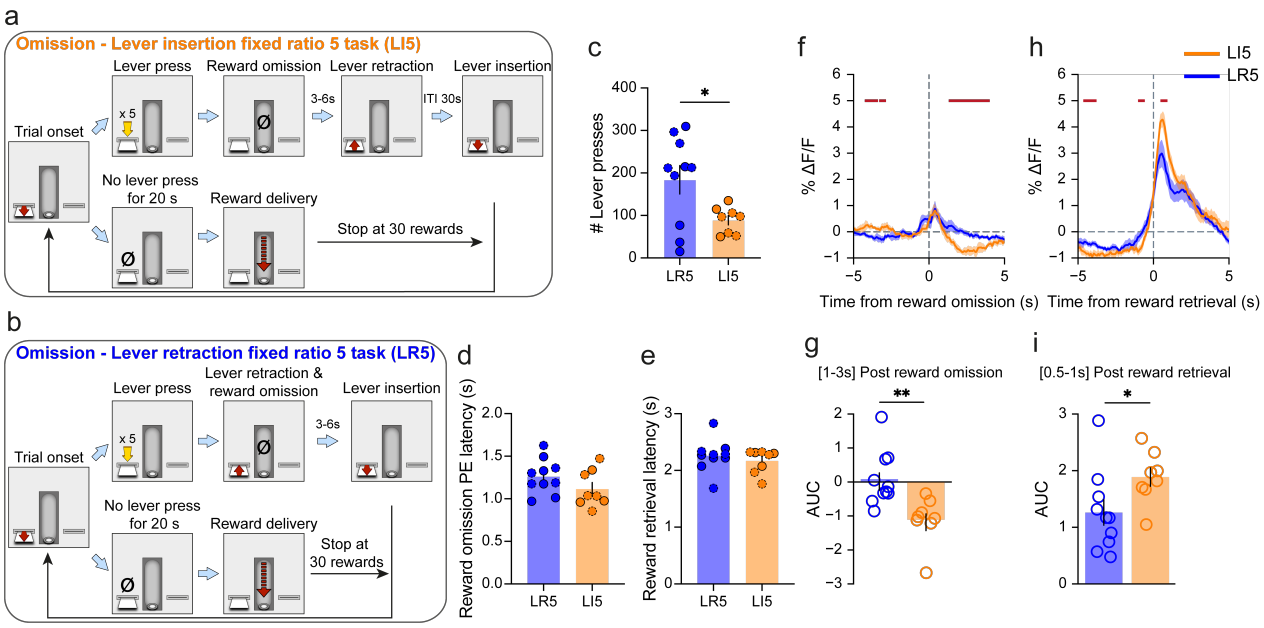

Figure 4. Behavioral inflexibility of LR5 rats during the omission test is associated with attenuated reward prediction error signals in the VTA. *(**a-b**) Omission test design for the LI5 task (**a**) and the LR5 task (**b**). (**c**) Total number of lever presses during the omission test (two-way ANOVA: task effect: $F_{1,17}$ = 6.58, p = 0.022; no task x sex interaction: $F_{1,17}$ = 2.9, p = 0.109). (**d**) Latency to enter the port after ratio completion and omission of the reward (two-way ANOVA: no task effect: $F_{1,17}$ = 2.08, p = 0.171; no task x sex interaction: $F_{1,17}$ < 1, p = 0.670). (**e**) Unexpected reward retrieval latency (two-way ANOVA: no task effect: $F_{1,17}$ < 1, p = 0.553; no task x sex interaction: $F_{1,17}$ < 1, p = 0.58). (**f**) Phasic VTA dopamine neuron activity around port entries following* omission of the reward. *(**g**) Area under the curves for 1 to 3 seconds after reward omission (unpaired two-tailed t-test comparison, t_{16}= 3.30, p = 0,004). (**h**) Phasic VTA neuron activity around retrieval of unexpected reward. (**i**) Area under the curves for 0.5 to 1 seconds after reward retrieval (unpaired two-tailed t-test comparison, t_{16}= -2.15, p = 0.047). Data shown as means ± SEM, superimposed with individual data point. LI5 n = 8 (3 male; 5 female); LR5 n = 10 (5 male; 5 female). Red horizontal bars indicate significant difference between LI5 and LR5 tasks at 95% confidence level. *p < 0.05; **p < 0.01.*

Distinct patterns of DA release in the nucleus accumbens core in response to cues, lever presses and reward

We next asked if the distinct patterns of VTA DA neuron activity we observed would be reflected in similar patterns of DA release in the nucleus accumbens core (NAc core), a primary target for VTA DA neurons that is implicated in DA-mediated cue processing and reward learning [33–36]. To this end, we infused the dopamine sensor dLight1.2 into NAc core in male and female rats (**Fig. 5a-b**).

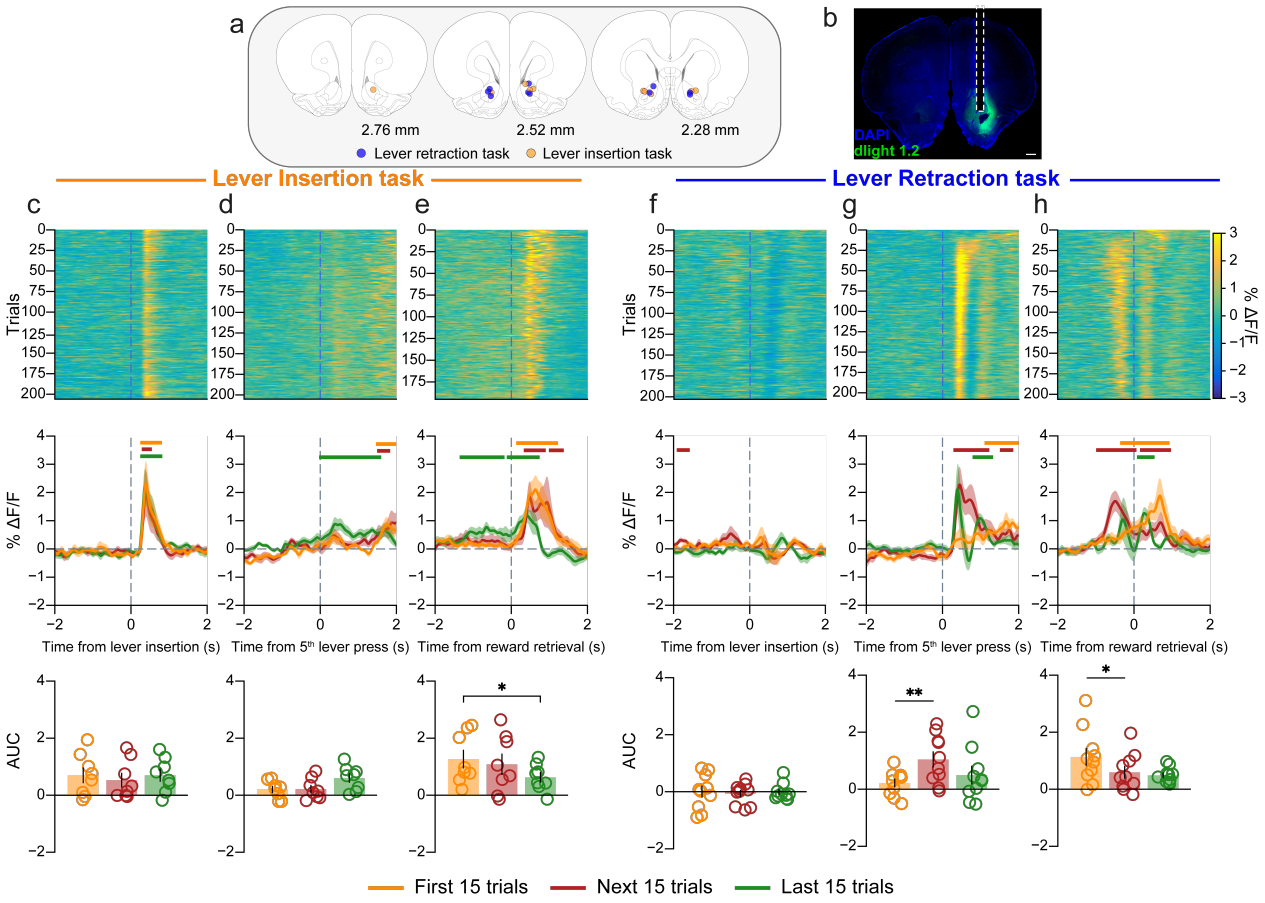

Figure 5. Dynamic changes in dopamine release in the NAc core in response to cues and reward in the two tasks. *(**a**) Coronal sections showing location of optic fiber tips relative to Bregma in LI5 and LR5 tasks. (**b**) dLight 1.2 was infused in the NAc core, and the optic fiber, represented with the white dash line, was implanted above the injection site. Scale bar: 500 µm. (**c**) Top panel: LI5 task heatmap displaying trial-by-trial dopamine release, averaged across rats, around lever insertion. Middle panel: phasic dopamine release around lever insertion averaged across rats and trials for the first 15 trials (orange line), the next 15 trials (red line) and the last 15 trials (green line) of training. Bottom panel: area under the curves (AUCs) for 0 to 1 seconds following lever insertion (two-way RM ANOVA, no trial x sex interaction $F_{2,12} = 1.18$, $p = 0.34$; no trial effect: $F_{2,12} < 1$, $p = 0.58$). (**d**) Same as c for the 5th lever press event in the LI5 task (two-way RM ANOVA, no trial x sex interaction $F_{2,12} < 1$, $p = 0.96$; trial effect: $F_{2,12} = 4.58$, $p = 0.033$; paired two-tailed t-test post-hoc comparison: corrected p-values > 0.05). (**e**) Same as c for reward retrieval in the LI5 task (two-way RM ANOVA, no trial x sex interaction $F_{2,12} < 1$, $p = 0.76$; trial effect: $F_{2,12} = 4.85$, $p = 0.03$; paired two-tailed t-test post-hoc comparison). (**f**) Same as c for lever insertion in the LR5 task (two-way RM ANOVA, no trial x sex interaction $F_{2,16} < 1$, $p = 0.9$; no trial effect: $F_{2,16} < 1$, $p = 0.88$). (**g**) Same as c for the 5th lever press in the LR5 task (two-way RM ANOVA, no trial x sex interaction $F_{2,16} < 1$, $p = 0.47$; trial effect: $F_{2,16} = 5.41$, $p = 0.016$; paired two-tailed t-test post-hoc comparison). (**h**) Same as c for reward retrieval in the LR5 task (two-way RM ANOVA, no trial x sex interaction $F_{2,16} < 1$, $p = 0.80$; trial effect: $F_{2,16} = 5.70$, $p < 0.014$; paired two-tailed t-test post-hoc comparison). Data shown as means ± SEM, superimposed with individual data point. LI5 n = 8 (3 males; 5 females); LR5 n = 10 (5 males; 5 females). Horizontal bars indicate significant deviation from baseline at 99% confidence level. *p < 0.05; **p < 0.01.*

Changes in patterns of DA release tended to mirror the observed changes in VTA DA neuron activity across training in the LI5 and LR5 tasks. Specifically, the lever insertion cue elicited a peak in DA release in the LI5 task (**Fig. 5c**) but not in the LR5 task (**Fig. 5f**). Conversely, the fifth lever press did not evoke DA activity in the LI5 task (**Fig. 5d**), while it caused a significant DA release in the LR5 task (**Fig. 5g**). In addition, we observed a prominent reward peak that somewhat diminished by the end of the training in the LI5 task (**Fig. 5e**), and, in contrast, a reward peak that rapidly shifted to the lever retraction cue in the LR5 task (**Fig. 5h**).

Consistent with measures of VTA DA neuron activity, we observed peaks of DA release during lever presses in the LI5 task but not in the LR5 task. These peaks did not change across training (**Suppl. Fig. 4**).

Together with the findings from VTA-GCaMP recordings, these results suggest that a shift in phasic DA signals from reward retrieval to the termination of the sequence occurs within the first session in the LR5 task (from the first 15 trials to the next 15 trials) in which lever retraction explicitly cues sequence completion and reward delivery, but not after extended training in the LI5 task in which no cue signals imminent reward delivery.

Inflexibility mediated by the lever retraction cue under an omission schedule is associated with attenuated negative RPE DA signals in the NAc core

We next monitored DA release in the NAc core under an omission schedule as before to determine how DA signaling in this region is affected when reward expectation is violated. We replicated our behavioral finding of lever pressing persistence in rats trained in the LR5 task compared to rats trained in the LI5 task (**Fig. 6a**). Again, we observed an attenuated decrease in DA signals when expected reward was omitted in rats trained in the LR5 task compared to rats trained in the LI5 task (**Fig. 6d-e**). However, we did not observe any difference in the DA responses to unexpected reward delivery (**Fig. 6f-g**). Similar to what we observed in the VTA-recorded rats, the differences in reward signals are unlikely to result from different motor response as the mean latency to enter the port after reward omission (**Fig. 6b**) or delivery (**Fig. 6c**) does not differ between LR and LI rats. These results indicate that the lever retraction cue-mediated inflexibility is associated with attenuation of the negative RPE DA signals in the NAc core of rats trained in the LR5 task.

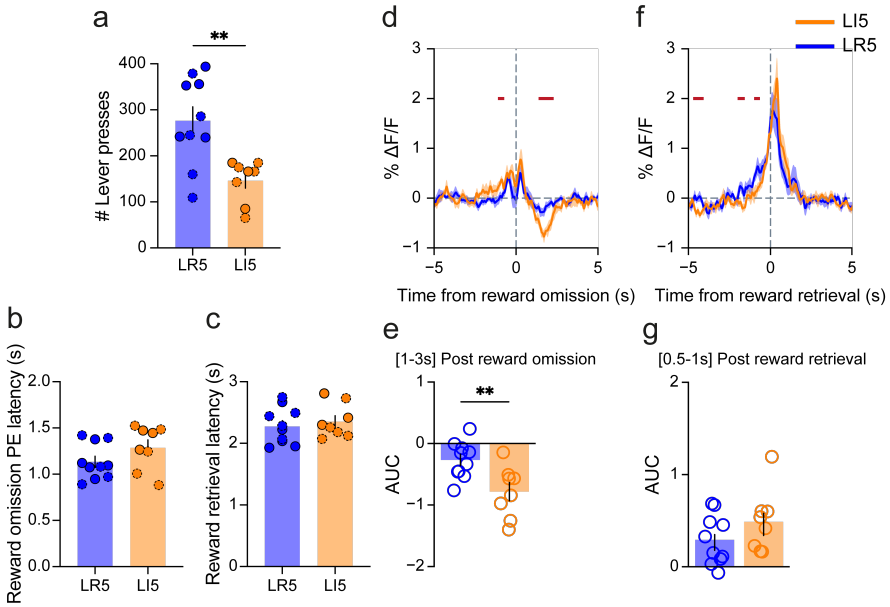

Figure 6. Lower behavioral flexibility of LR5 rats during the omission test is associated with attenuated negative reward prediction error-like signal in the NAc core. *(**a**) Total number of lever presses performed during the omission test (two-way ANOVA task effect: $F_{1,17}$ = 12.71, p = 0.003; no task x sex interaction: $F_{1,17}$ = 1.27, p = 0.277). (**b**) Latency to enter the port after ratio completion and omission of the reward (two-way ANOVA: no task effect: $F_{1,17}$ = 2.66, p = 0.125; no task x sex interaction: $F_{1,17}$ < 1, p = 0.378). (**c**) Unexpected reward retrieval latency (two-way ANOVA: no task effect: $F_{1,17}$ < 1, p = 0.435; no task x sex interaction: $F_{1,17}$ = 3.28, p = 0.091). (**d**) Phasic NAc core dopamine release around port entries following reward omission. (**e**) Area under the curves 1 to 3 seconds after omission (unpaired two-tailed t-test comparison, t_{16}= 3.07, p = 0,007). (**f**) Phasic NAc core dopamine signal around retrieval of unexpected reward. (**g**) Area under the curves 0.5 to 1 seconds after reward retrieval (unpaired two-tailed t-test comparison, t_{16}= -1.36, p = 0,191). Data are shown as means ± SEM, superimposed with individual data point. LI5 n = 8 (3 males; 5 females); LR5 n = 10 (5 males; 5 females). Red horizontal bars indicate significant difference between LI5 and LR5 tasks at 95% confidence level. *p < 0.05; **p < 0.01.*

Optogenetic VTA DA neuron stimulation at the time of sequence completion drives automaticity and behavioral chunking

Given our prior observation that lever retraction cues paired with reward delivery evoke phasic activity of VTA dopamine neurons and are associated with the development of both automaticity and behavioral chunking in LR5 rats, we sought to replicate this behavioral pattern by mimicking cue-elicited DA in an optogenetic experiment. TH-Cre$^+$ rats were unilaterally infused in the VTA with DIO-ChR2 or DIO-eYFP virus and implanted with an optic fiber (**Fig. 7a**). We modified the LI5 task (**Fig. 7b**) to incorporate brief optogenetic stimulation (0.5 s; 20 mW; 20 Hz) to artificially recreate the activity peak observed upon completion of the fifth lever press and lever retraction in the LR5 task. As with the original LI5 task, the lever remained extended until rats entered the port to consume the reward, preventing them from using the lever retraction as a reward-predictive cue.

Optogenetic stimulation resulted in a progressive increase in response rates in ChR2 rats as compared to eYFP rats receiving equal presentations of laser over training sessions (**Fig. 7c-d**). The distribution of inter-press intervals (IPI) was comparable between ChR2 and eYFP rats on the first session (**Fig. 7e**) but differed between groups by the last session (**Fig. 7f),** with a remarkable increase in the proportion of very short IPIs in ChR2 rats (**Fig. 7f insert**). These findings suggest that stimulating VTA DA neurons at sequence completion resulted in progressively faster sequence execution across training. In addition, optogenetic stimulation of VTA DA neurons resulted in a moderate but significant decrease in port checking across training sessions (**Fig. 7g**). Thus, all ChR2 rats exhibited a decrease in port entry likelihood between the first and last session (**Fig. 7h**). Finally, analysis of lever press sequence length revealed no difference between the two groups during the first session, with a majority of single presses in both eYFP and ChR2 rats (**Fig. 7i**, ~60%). However, on the last training session, eYFP rats persisted with recurrent port checking, whereas ChR2 rats reduced the proportion of single presses, tending to respond in bouts of 2 or 3 presses before checking the port (**Fig. 7j**).

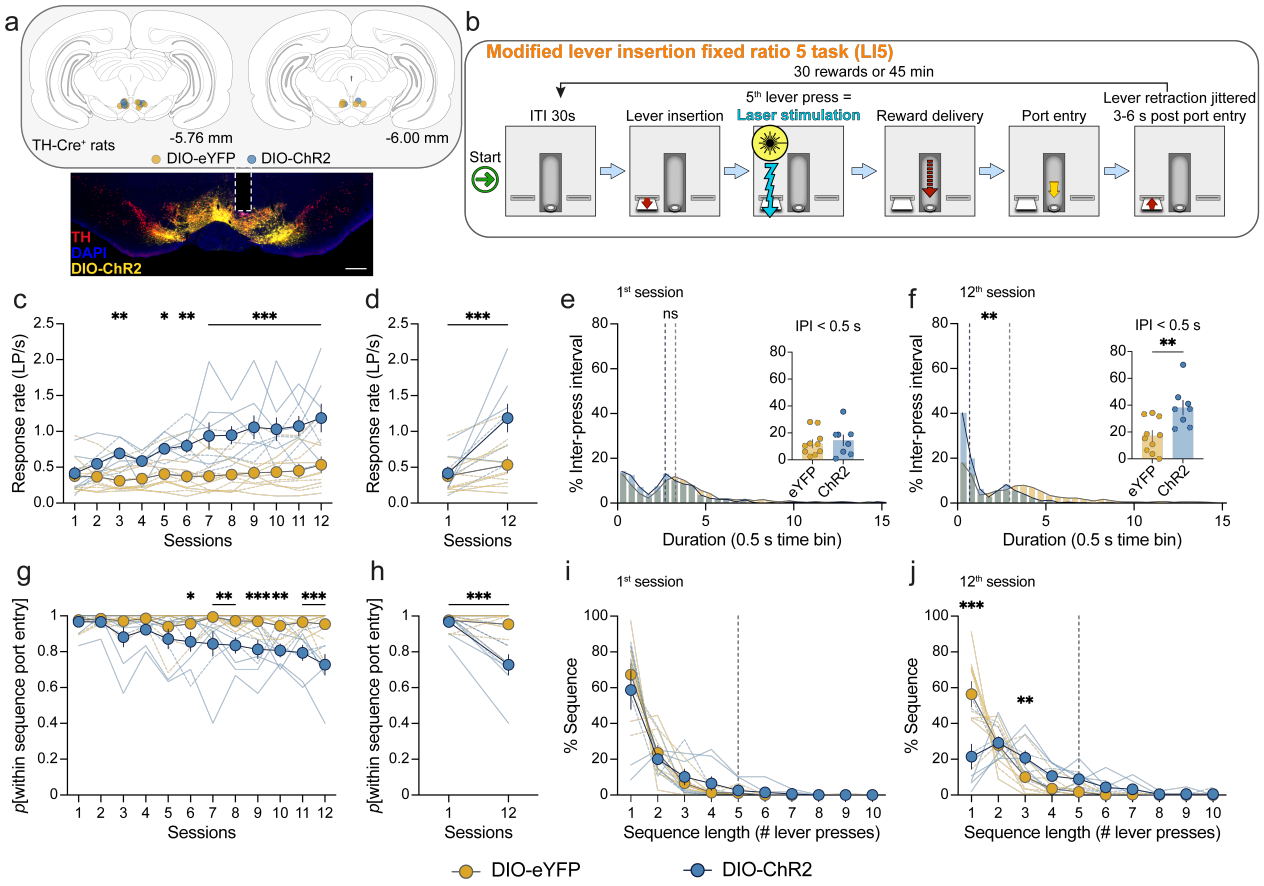

Figure 7. Optogenetic VTA DA neuron stimulation at the time of sequence completion drives automaticity and behavioral chunking. *(**a**) Targeting VTA DA neurons with DIO-eYFP or DIO-ChR2 virus in TH-Cre^{+} rats. Scale bar: 500µm. (**b**) Task design for optogenetic stimulation of VTA DA neurons at sequence completion (**c**) Response rate in lever press per second (LP/s) within the lever press sequence (two-way RM ANOVA, group x session interaction: $F_{11,154} = 4.64$, $p < 0.001$; group effect: $F_{1,14} = 17.26$, $p < 0.001$; no group x session x sex interaction $F_{11,154} = 1.55$, $p = 0.118$; Student Newman-Keuls post hoc pairwise comparison). (**d**) Response rate on the first versus last session (two-way RM ANOVA, group x session interaction: $F_{1,14} = 7.7$, $p = 0.015$; no group x session x sex interaction $F_{1,14} < 1$, $p = 0.36$; Student Newman-Keuls post hoc pairwise comparison). (**e**) Frequency distribution of inter-press intervals (IPI) for the first session in DIO-eYFP and DIO-ChR2 rats (Mann-Whitney Rank Sum t test median comparison U = 395, p = 0.23). Insert panel: individual proportion of IPI under 0.5 s (two-way ANOVA no group effect $F_{1,14} < 1$, $p = 0.65$; no group x sex interaction $F_{1,14} < 1$, $p = 0.52$). (**f**) Frequency distribution of inter-press intervals (IPI) for the last session in DIO-eYFP and DIO-ChR2 rats (Mann-Whitney Rank Sum t test median comparison U = 274, p = 0.004). Insert panel: individual proportion of IPI under 0.5 s (two-way ANOVA group effect $F_{1,14} = 11.1$, $p = 0.005$; no group x sex interaction $F_{1,14} = 2.09$, $p = 0.17$). (**g**) Probability to enter the port within the sequence (within-sequence port entry) (two-way RM ANOVA, group x session interaction: $F_{11,154} = 4.09$, $p < 0.001$; group effect: $F_{1,14} = 13.57$, $p < 0.001$; no group x session x sex interaction $F_{11,154} = 1.42$, $p = 0.166$; Student Newman-Keuls post hoc pairwise comparison). (**h**) Probability of within sequence port entry on the first versus last session in DIO-eYFP and DIO-ChR2 rats (two-way RM ANOVA, group x session interaction: $F_{1,14} = 19.88$, $p < 0.001$; no group x session x sex interaction $F_{1,14} = 2.88$, $p = 0.112$; Student Newman-Keuls post hoc pairwise comparison). (**i**) Frequency distribution of sequence length during the first training session. The grey dashed line represents the optimal sequence length of 5 lever presses*

*(two-way RM ANOVA, no group x sequence length interaction: $F_{9,126} < 1$, $p = 0.75$; no group effect: $F_{1,14} < 1$, $p = 0.54$; group x sequence length x sex interaction $F_{9,126} = 2.42$, $p = 0.014$). **(j)** Same as i for the last training session (two-way RM ANOVA, group x sequence length interaction: $F_{9,126} = 10.12$, $p < 0.001$; group effect: $F_{1,14} = 5.4$, $p = 0.036$; Student Newman-Keuls post hoc pairwise comparison). Data shown as mean ± SEM, superimposed with individual data point. DIO-eYFP n = 10 (5 males; 5 females); DIO-ChR2 n = 8 (4 males; 4 females). Solid line: males; dash line: females. *p < 0.05; **p < 0.01; ***p < 0.001.*

Although both groups obtained a similar number of rewards throughout training (**Suppl. Fig. 5a**), ChR2 rats exceeded the response requirement (**Suppl. Fig. 5b**) and retrieved the reward with a shorter latency than eYFP rats (**Suppl. Fig. 5c**). The tendency to exceed the response requirement could be interpreted as resulting from the reinforcing effect of VTA DA neuron stimulation [21,22,37]. However, with the exception of one rat, optogenetic stimulation of VTA DA neurons in ChR2 rats failed to support robust intra-cranial self-stimulation (ICSS) with the stimulation parameters used in this experiment (0.5 s; 20 mW; 20 Hz, in absence of cue) (**Suppl. Fig. 5d to f**), indicating that reinforcing effects of DA neuron stimulation do not account for the results reported here. Indeed, if rats were responding for DA neuron stimulation, a longer, not shorter, latency to retrieve reward would be expected. Importantly, robust ICSS was observed when laser stimulation was increased to 2s and was paired with a cue light, as shown previously [21,22,37] (**Suppl. Fig. 5g to i**). In sum, these findings show that brief unilateral VTA DA neuron activation is sufficient to promote behavioral chunking of action sequences.

DISCUSSION

In this study, we examined the role of phasic DA signals during performance of action sequences that were differentially impacted by sequence initiation and termination cues. Specifically, we found that a lever retraction cue marking sequence completion in the LR5 task facilitated habit-like behavior. Conversely, when the sequence completion cue was absent in the LI5 task, in which lever insertion acted as a cue to indicate the opportunity to perform actions for reward access, rats exhibited greater goal-directedness, without behavioral chunking, as indicated by active reward seeking between lever presses. These distinct response strategies were associated with differential changes in mesolimbic DA signals, which captured variations in reward expectation along the execution of action sequences in the LR5 and LI5 tasks. We also found that behavioral inflexibility in rats trained in the LR5 task was associated with blunted positive and negative RPE-like signals in an omission test. Finally, optogenetic stimulation of VTA DA neurons at sequence termination, immediately prior to reward delivery and in absence of the lever retraction cue, was sufficient to promote automaticity and behavioral chunking.

We have previously shown that lever cues at the boundaries of action sequences promote habit formation and behavioral chunking [11,12,17]. Here, we extended these findings by demonstrating that the lever retraction cue, but not the lever insertion cue, is sufficient to promote habit-like behavior. Indeed, rats trained in the LR5 task were more likely to show an insensitivity to outcome devaluation compared to those trained in the LI5 task. These LR5-trained rats also displayed higher automaticity in lever pressing, without reward expectation until completion of the sequence, which is indicative of behavioral chunking [10,38]. Finally, LR5 rats were less sensitive than LI5 rats to a reversal of instrumental contingency in the omission test, suggesting some form of behavioral inflexibility. These results support the hypothesis that the reward predictive cue (i.e. lever retraction) serves as response feedback that favors habit formation and behavioral chunking by alleviating the need for action monitoring [12]. Indeed, rats do not need to track progress during sequence execution [39] but can instead learn to continue pressing on the lever until its retraction. These findings are in agreement with prior studies showing that reward predictability favors habit

whereas a reduction in predictability is sufficient to restore goal-directed control [13–15,40–42].

Task differences in reward expectation along the behavioral sequence were associated with specific changes in DA signals across events and trials, and these changes were similar in the VTA and in the NAc core. In the LR5 task, we observed a rapid shift in DA signal from reward retrieval to the lever retraction cue [26–28]. Phasic DA activity at the lever retraction cue is consistent with the certain expectation of reward at the termination of the action sequence in this task. In contrast, DA neurons were not modulated around lever presses in the LR5 task, when there is no reward expectation or prediction due to behavioral chunking. Conversely, in the LI5 task, there is no cue at sequence completion to signal reward delivery. Thus, reward delivery remained unpredictable and associated with a sustained reward peak in DA signal across training. Importantly, LI5 rats' behavior was characterized by greater goal-directedness and regular port checking between individual lever presses, suggesting some form of reward expectation at initiation and during sequence execution. Interestingly, DA signals peaked after individual lever presses with a decay in activity from sequence initiation to sequence termination. Furthermore, the peak at sequence initiation followed the first lever press during early training, but preceded it after extended training. These results suggest that across training, rats learned to expect the reward after the lever insertion cue and at the approach of the lever, when they initiated the action sequence.

We found an attenuation of DA signals across training in the LR5 task but not in the LI5 task in VTA and NAc core. In the VTA, the DA neuron activity peak at the lever retraction cue was the highest on trials 16 to 30, suggesting that rats quickly learned the contingency between lever retraction and reward delivery. However, this activity decreased over subsequent trials, reaching low levels at both lever retraction and reward retrieval on the last 15 trials of the training. Interestingly, a prior study reported a similar phenomenon, where cue-induced DA release within the ventral striatum decreased as animals became expert in the task [27]. This decrease in activity cannot be attributed to an extinction of fluorescent signal over time since VTA DA neuron activity fully recovered following unexpected reward delivery in the omission test. Instead, it is possible that behavioral chunking and habit learning is accompanied by a progressive disengagement of the mesolimbic pathway (VTA-NAc) and increased engagement of the nigrostriatal pathway (SNc-Dorsal striatum) [43–48]. Indeed, the DA system is interconnected through spiraling loops with different subregions of the striatum [49,50] . The sequential shift in DA control from the mesolimbic to the nigrostriatal pathway has been suggested as a neural basis for the development of automaticity and the transition from goal-directed to habitual control [43,44,51]. However, recent findings showing that habitual behavior is associated with specific patterns of DA release in the DMS but not the DLS, are challenging this theory [30,52,53]. To directly test this hypothesis, future experiments should focus on recording neural activity in the SNc and DA release in subregions of the dorsal striatum.

The behavioral measures of automaticity and behavioral chunking we observed in lever retraction task (LR5) do not invariably indicate habitual control. In our prior work[39], we required rats to respond in a sequence of five consecutive lever presses without port checking to earn the reward, a behavior that required action monitoring and goal-directed control and yet resulted in highly efficient performance similar to that seen here in the LR group. The difference is that here LR rats had a feedback cue freeing them from the need to self-monitor, thereby promoting habit. Thus, the feedback cue is the critical feature for habitual strategy adoption in this task. This lever retraction feedback cue elicited a large DA transient in both VTA and NAc as rats learned. Optogenetically mimicking this DA feedback cue in rats without actual lever retraction biased behavior towards automaticity. Together, these findings emphasize the important role of a feedback cue at the completion of action sequences in promoting habit-like behavior.

DA signaling has been proposed to mediate credit assignment [54], i.e., the appropriate connection of a given action or set of actions with its outcome. Thus, a possible mechanism underlying the effect of optogenetic manipulation on our automaticity measures is that optogenetic DA stimulation reinforces actions preceding the stimulation, initially the final lever press of the sequence, and, over time via back propagation links together the relevant preceding presses[26,55]. Interestingly, rats that received DA stimulation at the time of sequence completion often exceeded the required number of lever presses to receive the reward. While this behavior could be mistaken for intra-cranial self-stimulation (ICSS), the brief (0.5s) stimulation of VTA DA neurons in our study does not exhibit the strong reinforcing properties typically associated with longer (1s) stimulation durations, as reported in other studies [21,22,37,56] (but see [57]). Despite this, the ChR2 rats remained engaged in the task, as evidenced by the number of rewards obtained throughout training and their short latency to retrieve rewards. Therefore, the additional lever presses likely indicate the difficulty in inhibiting a prepotent behavior due to an increased speed in sequence execution.

Although this manipulation reproduced the behavioral pattern observed in the LR5 task, the effect was only partial, with a reduced amplitude compared to the LR5 task. This reduced effect could be due to the limited population of VTA DA neurons activated by unilateral optogenetic stimulation in comparison with a larger population of these neurons that are activated in response to a salient reward predictive stimulus, the lever retraction. It would be interesting to further investigate whether behavioral chunking induced by stimulation of VTA DA neurons is associated with habit learning and behavioral inflexibility, as shown in the LR5 task.

During the omission test, DA activity reflected positive and negative RPE-like signals that were different in rats trained in the two tasks. Specifically, LR5 rats displayed less inhibition of VTA and NAc core DA signals following the omission of the reward after completion of the lever press sequence, compared to LI5 rats. Additionally, these LR5 rats also showed less of an increase in DA neuron activity when they entered the port to retrieved unexpected rewards than LI5 rats. This finding is in agreement with prior studies showing reduced DA signals following omission or devaluation of the reward [19,27]. Interestingly, while both positive and negative RPE signals were attenuated in rats trained in the LR5 task, the attenuation was more pronounced for the negative RPE associated with reward omission. This deficit in negative RPE signaling suggests an impaired ability to update current reward contingencies which may underlies reduced behavioral inhibition observed in LR5 rats as they persisted to press the lever despite reward omission.

To conclude, we have shown that sequence initiation and termination cues differentially affect reward expectation during action sequences, with the sequence termination cue specifically contributing to habit-like behavior. We observed that this habit-like behavior was reflected in behavioral inflexibility of rats trained in the LR5 task, which was associated with attenuated DA RPE signals. Finally, using optogenetics, we demonstrated the contribution of feedback cue elicited phasic DA activity in the development of habit-like behavior.

MATERIALS & METHODS

Subjects

Male and female Wild-Type (WT) or TH-Cre^{+} Long-Evans rats were used in this study. These rats express Cre recombinase under the control of the tyrosine hydroxylase (TH) promoter [58]. Rats were individually housed under a 12 h/light/dark cycle (lights ON at 7 am). They were food restricted to 90 % of free feeding weight, starting one week before training, but had *ad libitum* access to water throughout the experiment. All rats were 8 to 10 weeks old at the beginning of the experiment. These studies were carried out in accordance with the recommendations of the Guide for the Care and Use of Laboratory Animals (Institute of Instrumental Training Laboratory Animal Resources, Commission of Life Sciences, National Research Council, 1996). The protocol was approved by the animal care and use committee of Johns Hopkins University.

Behavioral training

Apparatus

The apparatus consisted of operant chambers (Med associates) each equipped with a retractable lever on the left side of the right wall. The reward (0.1mL of 20 % sucrose) was delivered over 3-s in a magazine equipped with an infra-red beam, and located next to the lever. The house-light, located on the back wall of the operant chamber remained illuminated for the length of the session.

Initial training

Rats experienced one magazine training session in which 30 sucrose rewards were delivered under a random interval 60 s schedule. The following days, they were trained to press the lever to earn reward on a fixed-ratio 1 (FR1) schedule. Sessions were limited to 1 hour or 30 reward deliveries, whichever occurred first. Rats were trained one session per day, for 3 to 5 sessions, until they earned the maximum 30 rewards in less than an hour. Rats were then trained on a FR5 schedule (five responses per reward) for 5 additional sessions, limited to 30min or 30 reward deliveries, whichever occurred first. During initial instrumental training, the lever was continuously presented and no cue indicated when reward was delivered.

LI5 and LR5 task design

The lever insertion fixed-ratio 5 (LI5) task and the lever retraction fixed-ratio 5 (LR5) task were designed such that only one of the lever cues (lever insertion or retraction, respectively) is relevant to signal reward while the other cue, is made irrelevant. Both groups of rats were trained in parallel in the LI5 task or LR5 task. Two rats were excluded from analyses because they omitted the reward more than 70% of the trials on average across the 12 sessions, leaving a total of 30 rats (LI5: n=15, 8 females, 7 males; LR5: n=15, 8 females, 7 males).

LI5 task

As detailed in **Fig 1a**, each trial begun with a 30-s inter-trial interval prior to the insertion of the lever in the cage. Rats were then required to press the lever five times to receive the reward. The fifth lever press triggered reward delivery, which was not signaled by the lever retraction cue. To ensure that rats did not pay attention to the retraction of the lever, this event occurred during reward consumption, at a random interval ranging from 3 to 6-s after rats' entry into the magazine or at the exit of the magazine, whichever occurred first. The session ended after 45-min or 30 reward deliveries. For each trial, the lever remained extended until the rats completed the ratio and entered the magazine to consume the sucrose.

LR5 task

As detailed in **Fig 1b**, each trial begun with the insertion of the lever in the cage. The completion

of the FR5 requirement led to the retraction of the lever which signaled reward delivery, occurring at the fifth lever press. To ensure that rats did not pay attention to the insertion of the lever, this event occurred at a random interval ranging from 3 to 6 s after the rats entered the magazine to consume the sucrose or at magazine exit, whichever occurred first. The session ended after 30-min or 30 reward deliveries. For each trial, the lever remained extended until completion of the ratio.

Outcome devaluation by sensory-specific satiety

Each rat received 2 days of testing, separated by one reinforced training session. Rats were given 1h free access to their training reward (sucrose 20%; devalued condition) or to a control reward, which never served as a reinforcer (grain-based pellet; valued condition). Pre-feeding occurred in feeding cages in the experimental room. Immediately after pre-feeding, rats were placed in the operant chambers for a test session conducted under extinction with the same LI5/LR5 task design. Test sessions were limited to 10 trials or 10 minutes of lever presentation, whichever occurred first. Experimental valued/devalued conditions were reversed for the second test session and the order of conditions was counterbalanced across rats.

Omission test

As illustrated in **Fig 4a-b** the omission schedule consisted on a single test session in which animals had to refrain from pressing the lever for 20 s in order to obtain the reward. In contrast, completion of the FR5 resulted in omission of the reward. Every lever press reset the 20-s timer. The fundamental structures of the LI5 and LR5 tasks were maintained: for rats trained in the LI5 task, lever insertion indicated the initiation of a trial, while for those trained in the LR5 task, lever retraction denoted the fulfillment of the response requirement. The session only ended after 30 rewards were delivered, with no time limit.

Surgical procedure

Surgeries for viral infusions and optic fiber implants were carried out as previously described [22,59]. Rats were anesthetized with 5% isoflurane and placed in a stereotaxic frame, after which anesthesia was maintained at 1–3%. Rats were administered carprofen anesthetic (5 mg/kg), and cefazolin antibiotic (70 mg/kg) subcutaneously. The top of the skull was exposed and holes were drilled for viral infusion, optic fiber implant, and four skull screws. Viral injections were made using a microsyringe pump at a rate of 0.1 µl/min. Syringes were left in place for 5-min, then raised 200 µm dorsal to the injection site, left in place for another 10 min, then removed slowly. Implants were secured to the skull with dental cement. Optogenetic manipulations commenced at least 4 weeks after surgery. A total of 5 to 6 weeks was allowed for virus expression prior to photometry recording.

Fiber photometry

For fiber photometry recording of VTA dopamine neurons bulk calcium imaging, 1 µl Cre-dependent GCaMP6f (AAVDJ-EF1a-DIO-GCaMP6f; titer 5.25×10^{12} particles/ml, Stanford University) was infused unilaterally into the VTA (AP -5.8 mm, ML ±0.7 mm, DV -7.9 mm relative to Bregma) of TH-Cre+ rats. In order to avoid residual florescence recording from SNc, low-auto-fluorescence optic fibers (400 µm diameter; 0.57 numerical aperture, Doric Lenses) were inserted with a ±10° angle, directed toward the VTA midline, just dorsal to the injection site (AP -5.8 mm, ML ±1.7 mm, DV -7.4 mm relative to Bregma). Fiber photometry recording of dopamine signaling in the NAc was achieved via infusion of the dopamine sensor dLight1.2 virus (pAAV5-hSyn-dLight1.2: titer 5-5.75 $\times 10^{12}$ particles/ml, addgene) in the NAc Core (AP +1.8 mm, ML ±1.7 mm,

DV -7 mm relative to Bregma) of WT rats. Optic fibers in the NAc Core were implanted at AP +1.8 mm, ML ±1.7 mm, DV -6.8 mm relative to Bregma.

Optogenetics

AAV5-Ef1a-DIO-ChR2-eYFP (titer 4–4.2 × 10^{12} particles/ml, University of North Carolina) or AAV5-EF1a-DIO-eYFP (titer 4–6 × 10^{12} particles/ml, University of North Carolina) were infused unilaterally (0.7 µl at each target site, for a total of 2.8 µl per rat, as previously described [21,22]) at the following coordinates from Bregma for targeting VTA cell bodies: AP -6.2 and -5.4 mm, ML ±0.7 mm, DV -8.5 and -7.5. Custom-made optic fiber implants (300-µm glass diameter) were inserted unilaterally in the VTA, just above and between viral injection sites at the following coordinates relative to Bregma: AP -5.8 mm, ML ±0.7 mm, DV -7.5.

Fiber photometry recording

We assessed VTA dopamine neuron activity in TH-Cre^{+} rats during training in the LI5 task (n = 8; 5 females, 3 males) or the LR5 task (n = 10; 5 females, 5 males). Dopamine release in the NAc Core was assessed in WT rats trained in the LI5 task (n = 8, 5 females, 3 males) or the LR5 task (n = 10, n= 5 females, 5 males). For the group of rat recorded in the VTA, 3 LI5 trained and 6 LR5-trained did not experienced a jittered insertion of the lever in the cage. Instead, for the LI5 trained rats, the lever was retracted in the cage 0.5s after the port entry following ratio completion. For the LR5-trained rats, the lever was inserted in the cage 1.5s after the port entry following ratio completion.

Operant chambers were equipped with a real-time fiber photometry recording system (Tucker-Davis Technologies). A fluorescence mini-cube (Doric Lenses) was utilized to transmit light streams from a 465-nm LED modulated at 211 Hz and a 405-nm LED modulated at 531 Hz. The 465-nm LED passed through a GFP excitation filter, while the 405-nm LED passed through a 405-nm bandpass filter. The power of the LEDs was set at approximately 100 µW. These light sources were connected to an optic fiber implanted in the rat's brain. Power output was daily measured at the tip of the patch cord, before and after each rat's session to ensure a stable power across rats and recording days.
Both GCaMP6f and dLight fluorescence emitted by neurons below the fiber tip were captured by the mini-cube and passed through a GFP emission filter. The fluorescence signal was then amplified and focused onto a high sensitivity photoreceiver (Newport, Model 2151). To account for bleaching and movement artifacts, the brightness produced by the 465-nm excitation, which stimulates calcium-dependent GCaMP6f fluorescence, was demodulated and compared to the isosbestic 405-nm excitation, which stimulates GCaMP6f or dLight in a calcium and dopamine-independent manner.
Rats received initial operant training under the FR1 schedule before surgery Five to six weeks after virus infusion, rats were given two FR1 reminder sessions to acclimate rats to patch cord tethering and ensure they were able to move easily. Photometry recording was conducted throughout 8 training sessions in the LI5 and LR5 tasks and during the omission test.

Optogenetic stimulation

Optogenetic stimulation in the modified-LI5 task

Illumination was provided by 473-nm lasers (OptoEngine), adjusted to read 20 mW from the tip of the patch cord at constant illumination. Light power was measured before and after every behavioral session to ensure that laser power was constant within session. Black tape was wrapped around the ceramic sleeve used to connect the patch cord and the implanted optic fiber

to block visible light transmission that could be used as a cue during the task. A total of 8 ChR2 rats (4 females, 4 males) and 10 eYFP (5 females, 5 males) were run in this experiment. As shown in **Fig 7b**, the LI5 task was modified to include a brief laser stimulation (0.5-s; 20 Hz, 5-ms pulse duration) at the 5th lever press. Rats were trained for 12 consecutive sessions that terminated after 45 minutes or 30 rewards obtained.

Intra-cranial self-stimulation (ICSS)

At the end of the optogenetic experiment, all rats were tested for ICSS with the stimulation parameters used in the modified-LI5 task to assess the possible reinforcing effect of the laser stimulation. During 8 1-h daily sessions, rats had access to two nosepoke ports; a response at the active nosepoke resulted in delivery of a 0.5-s train of light pulses (20 Hz, 5-ms pulse duration). Inactive nosepokes were recorded but had no consequence. Eight additional 1-h ICSS sessions were conducted in which a response in the active nosepoke resulted in a 2-s laser stimulation (20 Hz, 5-ms duration) paired with a cue light in the active nosepoke. Correct ICSS in these conditions (above 150 responses at the active nosepoke) was used as criteria for rats' inclusion in the optogenetic experiment, in addition to correct virus expression and optic fiber placement in the VTA.

Tissue collection

Rats were deeply anesthetized with sodium pentobarbital and transcardially perfused with cold phosphate buffered (PB) saline (PBS) followed by 4 % paraformaldehyde (PFA). Brains were removed and post-fixed overnight in 4 % PFA. Brains were then cryoprotected in a PB solution containing 30 % sucrose for at least 48 h, frozen into liquid isopentane and store at -80°C until processed for histology.

Histology

Brains were processed into 50µm-thick coronal sections on a cryostat (Leica Microsystems). To verify viral expression of dLight and optic fiber placement, brain slices were directly mounted on microscope slide and coverslipped with Vectashield mounting medium containing DAPI. Brain sections were then imaged with a Zeiss Axio 2 microscope. To verify viral GCaMP, ChR2 and eYFP expression in midbrain dopamine neurons, we performed immunohistochemistry for tyrosine hydroxylase (TH) and GFP (for GCaMP only). Sections were washed in PBS and incubated with bovine serum albumin (BSA) and Triton X-100 (each 0.2 %) for 20 min. 10 % normal donkey serum (NDS) was added for a 30 min incubation, before primary antibody incubation (mouse anti-GFP, 1:1500, Invitrogen; rabbit anti-TH, 1:500, Fisher Scientific) overnight at 4 °C in PBS with BSA and Triton X-100 (each 0.2 %). Sections were then washed with PBS and incubated with 2 % NDS in PBS for 10 min. Secondary antibodies were added (1:200 Alexa Fluor 488 donkey anti-mouse; 1:200 594 donkey anti-rabbit, Invitrogen) for 2 h at room temperature. Sections were then washed in PBS and in PB and mounted with Vectashield mounting medium containing DAPI. Fluorescence as well as optic fiber tracks were then visualized. In order to determine the specific targeting of TH-Cre$^+$ neurons by DIO-viruses, 20 x three-channel images along the medial-lateral and anterior-posterior gradients of the midbrain were taken, using equivalent exposure and threshold settings. With the TH channel turned off, GFP$^+$ or eYFP$^+$ cells were first identified by a clear ring around DAPI-stained nuclei. The TH channel was then overlaid, and the proportion of GFP$^+$ or eYFP$^+$ cells co-expressing TH below optic fiber placements was counted.

Statistical analysis

Behavioral analysis

Data were subjected to three-way repeated measures analyses of variance (session as within-factor and task and sex as between-subject factors), followed by post-hoc comparisons when indicated, using Student Newman-Keuls pairwise comparison. Significance was assessed against a type I error rate of 0.05. Behavioral data that did not follow a normal distribution were analyzed using non parametric tests (Mann-Whitney Rank Sum t test for group comparison). Statistical tests were conducted on SigmaStat (Systat software Inc., San Jose, USA) and SPSS (IBM, Amorak, NY).

Analysis of photometry recordings

- ***Signal acquisition***

A real-time signal processor (RP2.1, Tucker-Davis Technologies) running Synapse software was used to modulate the output of each LED and record the photometry signals. The signals were sampled from the photodetector at a rate of 6.1 kHz and demodulated and decimated to 1017 Hz before being saved to disk. For analysis purposes, both signals were downsampled to 102 Hz, and a least-squares linear fit was applied to the 405-nm signal to align it with the 465-nm signal. This fitted 405-nm signal served as the reference for normalizing the 465-nm signal using the formula % ΔF/F =100 * (465-nm signal – fitted 405-nm signal)/(fitted 405-nm signal).

- ***Main analysis across trials during training***

For LI5/LR5 tasks, all ΔF/F photometry traces were analyzed from -2 to 2 s around each event of the behavioral sequence comprising the lever insertion (LI), the sequence of lever presses (LP1 to LP5) and the port entry (PE; reward retrieval). To analyze rapid changes in activity across training sessions, trials from all recording sessions were concatenated and the mean activity across the first 15 trials, the next 15 trials (trials 16-30) and the last 15 trials was compared for each task. Unless otherwise specified, the area under the curve (AUC) was computed from 0 to 1-s post-event. For statistical analysis, two-way repeated measure ANOVAs (trial set as within-subject factor and sex as between-subject factor) were conducted. Deviation from baseline (%dF/F ≠ 0) was determined via bootstrapped confidence intervals (99% or 95% CIs) as described in [60]. A consecutive threshold of 17 consecutive 10-ms time bins was applied for statistical evaluation.

- ***Deconvolution analysis***

For analysis purposes, both signals were downsampled to 25 Hz. In order to isolate response to each behavioral event (lever presses and reward retrieval), kernels were calculated as previously described [61]: time-dependent GCaMP6f signal was modeled as the sum of the response to each behavioral event. Calcium response to each event was computed as the convolution of a time series representing the time of the event (series of 0s and 1s, in which 1s correspond to the event timestamp) and to the kernel corresponding to the response profile to that event. The model can be written as follows, where g(t) is the GCaMP6f signal, where a, b, etc., are example of behavioral event time series, and where k^a and k^b are the kernels for the corresponding event:

$$g(t) = g0 + \sum_{t'=-1s}^{2s} a(t-t')k^a(t') + \sum_{t'=-1s}^{2s} b(t-t')k^b(t') + \cdots + error$$

For each recording session, the coefficients of the kernels were solved using the method of least-squares in Python (LinearRegression from sklearn package). **Suppl. Fig. 3** displays individual rats' kernel across the first and last recording sessions in the LI5 and LR5 tasks.

To identify when the signal significantly deviated from baseline, we used bootstrapping to obtain the 99% confidence interval and applied the consecutive thresholds method [60]. More specifically, the lower and upper bound of the confidence interval must be above or below 0 for a least 5 consecutive 40-ms time bins to detect statistical deviation from baseline.

- ***Analysis of GCaMP6f and dLight signal under omission schedule***

Photometry traces of % ΔF/F were analyzed within a time window of -5 to 5 seconds around two key events: the port entry that followed a reward omission or unexpected reward delivery. We computed the AUC from 0.5 to 1 second after the reward retrieval. To capture the delayed signal depression following the omission of the reward, we also calculated the AUC from 1 to 3 seconds after omission. To identify significant differences between the LI5 and LR5 tasks as shown in **Fig. 4** and **Fig. 6**, we conducted a comparison of peri-event waveforms between the two tasks, using the two-sample t-test and bootstrap technique (bootstrap difference distribution of randomly resampled means) as described in [60]. Deviation from baseline (%dF/F ≠ 0) was determined via bootstrapped confidence intervals (95% CIs) as described in [60]. A consecutive threshold of 17 consecutive 10-ms time bins was applied for statistical evaluation of differences between tasks and from baseline.

ACKNOWLEDGEMENTS

The authors thank all members of the Janak lab for their helpful discussions on the experimental findings.

FUNDING AND DISCLOSURES

This work was supported by NIH grant R01DA035943 (PHJ) and IRESP grant AAPSPA2021-V1-07 (NT). The authors declare no conflict of interest.

AUTHOR CONTRIBUTIONS

RM, YV and PHJ designed the experiments; RM, YV, collected the data with technical assistance from JZ and HP; RM, YV analyzed the data with assistance from YC on deconvolution analysis; RM, YV and PHJ interpreted the data and wrote the manuscript with inputs from all authors.

REFERENCES

1. Dickinson, A. Actions and Habits: The Development of Behavioural Autonomy. *Philosophical Transactions of the Royal Society* **308**, 67–78 (1985).
2. Watson, P. & de Wit, S. Current limits of experimental research into habits and future directions. *Curr Opin Behav Sci* **20**, 33–39 (2018).
3. Vandaele, Y. & Janak, P. H. Defining the place of habit in substance use disorders. *Prog Neuropsychopharmacol Biol Psychiatry* (2017) doi:10.1016/j.pnpbp.2017.06.029.
4. Du, Y., Krakauer, J. W. & Haith, A. M. The relationship between habits and motor skills in humans. *Trends Cogn Sci* **26**, 371–387 (2022).
5. Haith, A. M. & Krakauer, J. W. The multiple effects of practice: skill, habit and reduced cognitive load. *Curr Opin Behav Sci* **20**, 196–201 (2018).
6. Crego, A. C. G. *et al.* Complementary control over habits and behavioral vigor by phasic activity in the dorsolateral striatum. *Journal of Neuroscience* **40**, 2139–2153 (2020).

7. Dezfouli, A. & Balleine, B. W. Actions, Action Sequences and Habits: Evidence That Goal-Directed and Habitual Action Control Are Hierarchically Organized. *PLoS Comput Biol* **9**, e1003364 (2013).
8. Balleine, B. W. & Dezfouli, A. Hierarchical Action Control: Adaptive Collaboration Between Actions and Habits. *Front Psychol* **10**, (2019).
9. Dezfouli, A. & Balleine, B. W. Habits, action sequences and reinforcement learning. *Eur J Neurosci. 2012 Apr;35(7):1036-51. doi: 10.1111/j.1460-9568.2012.08050.x.* (2012).
10. Graybiel, A. M. The Basal Ganglia and Chunking of Action Repertoires. *Neurobiol Learn Mem* **136**, 119–136 (1998).
11. Vandaele, Y., Pribut, H. J. & Janak, P. H. Lever insertion as a salient stimulus promoting insensitivity to outcome devaluation. *Front Integr Neurosci* **11**, 1–13 (2017).
12. Vandaele, Y. & Janak, P. H. Lack of action monitoring as a prerequisite for habitual and chunked behavior: Behavioral and neural correlates. *iScience* **26**, 105818 (2023).
13. Bouton, M. E. Context, attention, and the switch between habit and goal-direction in behavior. *Learn Behav* **49**, 349–362 (2021).
14. Thrailkill, E. A., Michaud, N. L. & Bouton, M. E. Reinforcer predictability and stimulus salience promote discriminated habit learning. *J Exp Psychol Anim Learn Cogn* **47**, 183–199 (2021).
15. Thrailkill, E. A., Trask, S., Vidal, P., Alcalá, J. A. & Bouton, M. E. Stimulus control of actions and habits: A role for reinforcer predictability and attention in the development of habitual behavior. *J Exp Psychol Anim Learn Cogn* **44**, 370–384 (2018).
16. Turner, K. M. & Balleine, B. W. Stimulus control of habits: Evidence for both stimulus specificity and devaluation insensitivity in a dual-response task. *J Exp Anal Behav* (2023) doi:10.1002/jeab.898.
17. Vandaele, Y. *et al.* Distinct recruitment of dorsomedial and dorsolateral striatum erodes with extended training. *Elife* **8**, 1–29 (2019).
18. Glimcher, P. W. Understanding dopamine and reinforcement learning: the dopamine reward prediction error hypothesis. *Proc Natl Acad Sci U S A* **108 Suppl**, 15647–15654 (2011).
19. Schultz, W., Dayan, P. & Montague, P. R. A neural substrate of prediction and reward. *Science (1979)* **275**, 1593–1599 (1997).
20. Keiflin, R. & Janak, P. H. Dopamine Prediction Errors in Reward Learning and Addiction: From Theory to Neural Circuitry. *Neuron* **88**, 247–263 (2015).
21. Keiflin, R., Pribut, H. J., Shah, N. B. & Janak, P. H. Ventral Tegmental Dopamine Neurons Participate in Reward Identity Predictions. *Current Biology* **29**, 93-103.e3 (2019).
22. Saunders, B. T., Richard, J. M., Margolis, E. B. & Janak, P. H. Dopamine neurons create Pavlovian conditioned stimuli with circuit-defined motivational properties. *Nat Neurosci* **21**, 1072–1083 (2018).
23. Watabe-Uchida, M., Eshel, N. & Uchida, N. Neural Circuitry of Reward Prediction Error. *Annu Rev Neurosci* **40**, 373–394 (2017).
24. Engelhard, B. *et al.* Specialized coding of sensory, motor and cognitive variables in VTA dopamine neurons. *Nature* **570**, 509–513 (2019).
25. Fiorillo, C. D., Newsome, W. T. & Schultz, W. The temporal precision of reward prediction in dopamine neurons. *Nat Neurosci* **11**, 966–973 (2008).
26. Fraser, K. M., Pribut, H. J., Janak, P. H. & Keiflin, R. From Prediction to Action: Dissociable Roles of Ventral Tegmental Area and Substantia Nigra Dopamine Neurons in Instrumental Reinforcement. *Journal of Neuroscience* **43**, 3895–3908 (2023).
27. Collins, A. L. *et al.* Dynamic mesolimbic dopamine signaling during action sequence learning and expectation violation. *Sci Rep* **6**, 1–15 (2016).

28. Wassum, K. M., Ostlund, S. B. & Maidment, N. T. Phasic mesolimbic dopamine signaling precedes and predicts performance of a self-initiated action sequence task. *Biol Psychiatry* **71**, 846–854 (2012).
29. Hamid, A. A. *et al.* Mesolimbic dopamine signals the value of work. *Nat Neurosci* **19**, 117–126 (2015).
30. Phillips, C. D., Hodge, A. T., Myers, C. C., Leventhal, D. K. & Burgess, C. R. Striatal dopamine contributions to skilled motor learning. *J Neurosci* e0240242024 (2024) doi:10.1523/JNEUROSCI.0240-24.2024.
31. Howe, M. W., Tierney, P. L., Sandberg, S. G., Phillips, P. E. M. & Graybiel, A. M. Prolonged dopamine signalling in striatum signals proximity and value of distant rewards. *Nature* **500**, 575–579 (2013).
32. Kim, H. R. *et al.* A Unified Framework for Dopamine Signals across Timescales. *Cell* **183**, 1600-1616.e25 (2020).
33. Di Chiara, G. Nucleus accumbens shell and core dopamine: differential role in behavior and addiction. *Behavioural Brain Research* **137**, 75–114 (2002).
34. Fraser, K. M. & Janak, P. H. Long-lasting contribution of dopamine in the nucleus accumbens core, but not dorsal lateral striatum, to sign-tracking. *Eur J Neurosci* **46**, 2047–2055 (2017).
35. Wassum, K. M., Ostlund, S. B., Loewinger, G. C. & Maidment, N. T. Phasic mesolimbic dopamine release tracks reward seeking during expression of Pavlovian-to-instrumental transfer. *Biol Psychiatry* **73**, 747–755 (2013).
36. Saunders, B. T. & Robinson, T. E. The role of dopamine in the accumbens core in the expression of Pavlovian-conditioned responses. *Eur J Neurosci* **36**, 2521–2532 (2012).
37. Steinberg, E. E. *et al.* A causal link between prediction errors, dopamine neurons and learning. *Nat Neurosci* **16**, 966–973 (2013).
38. Graybiel, A. M. & Grafton, S. T. The striatum: Where skills and habits meet. *Cold Spring Harb Perspect Biol* **7**, 1–14 (2015).
39. Vandaele, Y., Ottenheimer, D. J. & Janak, P. H. Dorsomedial striatal activity tracks completion of behavioral sequences. *eNeuro* 2021.04.01.437899 (2021) doi:10.1101/2021.04.01.437899.
40. Trask, S., Shipman, M. L., Green, J. T. & Bouton, M. E. Some factors that restore goal-direction to a habitual behavior. *Neurobiol Learn Mem* **169**, (2020).
41. Bouton, M. E., Broomer, M. C., Rey, C. N. & Thrailkill, E. A. Unexpected food outcomes can return a habit to goal-directed action. *Neurobiol Learn Mem* **169**, (2020).
42. Turner, K. M. & Balleine, B. W. Stimulus control of habits: Evidence for both stimulus specificity and devaluation insensitivity in a dual-response task. *J Exp Anal Behav* (2023) doi:10.1002/jeab.898.
43. Keramati, M. & Gutkin, B. Imbalanced Decision Hierarchy in Addicts Emerging from Drug-Hijacked Dopamine Spiraling Circuit. *PLoS One* **8**, (2013).
44. Lerner, T. N. Interfacing behavioral and neural circuit models for habit formation. *J Neurosci Res* **98**, 1031–1045 (2020).
45. Belin, D. & Everitt, B. J. Cocaine Seeking Habits Depend upon Dopamine-Dependent Serial Connectivity Linking the Ventral with the Dorsal Striatum. *Neuron* **57**, 432–441 (2008).
46. Belin, D., Jonkman, S., Dickinson, A., Robbins, T. W. & Everitt, B. J. Parallel and interactive learning processes within the basal ganglia: relevance for the understanding of addiction. *Behav Brain Res* **199**, 89–102 (2009).
47. Ambrosi, P. & Lerner, T. N. Striatonigrostriatal circuit architecture for disinhibition of dopamine signaling. *Cell Rep* **40**, (2022).
48. Yang, H. *et al.* Nucleus Accumbens Subnuclei Regulate Motivated Behavior via Direct Inhibition and Disinhibition of VTA Dopamine Subpopulations. *Neuron* **97**, 434-449.e4 (2018).

49. Haber, S. N., Fudge, J. L. & McFarland, N. R. Striatonigrostriatal pathways in primates form an ascending spiral from the shell to the dorsolateral striatum. *Journal of Neuroscience* **20**, 2369–2382 (2000).
50. Ikemoto, S. Brain reward circuitry beyond the mesolimbic dopamine system: A neurobiological theory. *Neurosci Biobehav Rev* **35**, 129–150 (2010).
51. Wickens, J. R., Horvitz, J. C., Costa, R. M. & Killcross, S. Dopaminergic mechanisms in actions and habits. *Journal of Neuroscience* **27**, 8181–8183 (2007).
52. Seiler, J. L. *et al.* Dopamine signaling in the dorsomedial striatum promotes compulsive behavior. *Current Biology* **32**, 1175-1188.e5 (2022).
53. van Elzelingen, W. *et al.* Striatal dopamine signals are region specific and temporally stable across action-sequence habit formation. *Current Biology* **32**, 1163-1174.e6 (2022).
54. Yagishita, S. *et al.* A critical time window for dopamine actions on the structural plasticity of dendritic spines. *Science* **345**, 1616–1620 (2014).
55. Tang, J. C. Y. *et al.* Dynamic behaviour restructuring mediates dopamine-dependent credit assignment. *Nature 2023 626:7999* **626**, 583–592 (2023).
56. Pascoli, V., Terrier, J., Hiver, A. & Lüscher, C. Sufficiency of Mesolimbic Dopamine Neuron Stimulation for the Progression to Addiction. *Neuron* **88**, 1054–1066 (2015).
57. Millard, S. J. *et al.* Cognitive representations of intracranial self-stimulation of midbrain dopamine neurons depend on stimulation frequency. *Nature Neuroscience 2024 27:7* **27**, 1253–1259 (2024).
58. Witten, I. B. *et al.* Recombinase-driver rat lines: Tools, techniques, and optogenetic application to dopamine-mediated reinforcement. *Neuron* **72**, 721–733 (2011).
59. Steinberg, E. E. *et al.* Positive reinforcement mediated by midbrain dopamine neurons requires D1 and D2 receptor activation in the nucleus accumbens. *PLoS One* **9**, (2014).
60. Jean-Richard-dit-Bressel, P., Clifford, C. W. G. & McNally, G. P. Analyzing Event-Related Transients: Confidence Intervals, Permutation Tests, and Consecutive Thresholds. *Front Mol Neurosci* **13**, (2020).
61. Parker, N. F. *et al.* Reward and choice encoding in terminals of midbrain dopamine neurons depends on striatal target. *Nat Neurosci* **19**, 845–854 (2016).